J. Opt. A: Pure Appl. Opt. **7** (2005) 767–773 doi:10.1088/1464-4258/7/12/010

Focusing of a train of pulses in phase opposition through a linear dispersive medium

Laura Chantada[1,4], Carlos R Fernández-Pousa[2], Maria Teresa Flores-Arias[1,4] and Carlos Gómez-Reino[3,4]

[1] Grupo de Óptica GRIN, Departamento de Física Aplicada, Escola Universitaria de Óptica e Optometría and Facultade de Física, Universidade de Santiago de Compostela, Campus Sur s/n, E15782 Santiago de Compostela (A Coruña), Spain
[2] División de Óptica, Departamento de Ciencia y Tecnología de Materiales, Universidad Miguel Hernández, Avenida Ferrocarril s/n, E03202 Elche (Alicante), Spain
[3] Signal Theory and Communications, Uni. Miguel Hernández, Avda. Universidad s/n Edificio Torrepinet, E03202 Elche (Alicante), Spain

E-mail: falaura@usc.es (L Chantada)

Received 13 April 2005, accepted for publication 13 October 2005
Published 15 November 2005
Online at stacks.iop.org/JOptA/7/767

Abstract
There exists a well known analogy between paraxial or one-dimensional Fresnel diffraction and the propagation of pulses in linear dispersive medium with negligible attenuation. Under this analogy, the envelope of a pulse is equivalent to the distribution of complex amplitude of the light in diffraction. In this context, we study the propagation of a train of identical Gaussian chirped pulses arranged in time in the same way as the Fresnel zones of a phase zone plate, in a highly dispersive guiding medium. From this study we find that the input train concentrates into a single pulse for certain values of total dispersion. We establish the focusing condition and characterize the output signal through its width and peak intensity, showing their dependences on the parameters that define the input train and the dispersive device.

Keywords: pulse propagation, pulse compression, dispersive propagation, zone plates

1. Introduction

There exists a well known analogy between paraxial diffraction and the propagation of pulses in a linear dispersive medium [1–5]. Under this analogy, the envelope of a pulse is equivalent to the distribution of the complex amplitude of light, dispersion is equivalent to diffraction, and linear chirping or quadratic phase modulation is equivalent to a lens [6]. The design and demonstration of devices based on this analogy is an active research topic due to their applications in pulse characterization and conformation. Dispersive lines together with modulators can be used to compress [7, 8], magnify [9–11] or retime [12] pulses individually. Pulse trains can be obtained from phase-modulated CW radiation [13, 14], and the use of dispersion to map the pulse profile into the Fourier domain [15, 16] has also been demonstrated, providing an all-optical method for time to frequency conversion [17, 18]. In these devices, dispersion acts on the pulses individually, and the subsequent result is a certain transformation of the input pulse. Coherence is only required within a single pulse or a single modulation cycle.

When the optical envelope is carried by a coherent wave, dispersion can provide new methods to perform optical tasks onto a signal composed of several pulses or a modulated wave. Dispersive propagation of CW light from laser diodes is a method to decrease [19] and characterizes its intensity noise, in this case after external phase modulation [20]. Temporal gratings have been used to obtain compressed pulses [21], and the temporal Talbot effect is a method for repetition rate

[4] http://www.usc.es/grinteam

multiplication of pulse trains [22–24]. Reshaping [25] and compression [26] in conjunction with coherent repetition rate multiplication have also been demonstrated.

In this context, our objective in this paper is to explore the possibility of temporal focusing of coherent pulse structures after dispersive propagation, in the same way as the Fresnel zones of a phase zone plate produce spatial focusing [27]. For certain values of the accumulated dispersion, a focused pulse is obtained without using any time lens, due to the progressive separation of the pulses in the input signal and the coherence of the underlying optical carrier. The idea is to exploit this analogy to increase the pulse peak intensity by means of dispersion. This linear method of pulse focusing is therefore different from the standard linear pulse compression technique, where phase modulation of a single pulse is combined with its propagation along a dispersion medium [7, 8], the advantage being that higher peak intensities can be obtained by coherent addition of a number of input pulses. To simplify our analysis, the train is assumed to be composed of identical Gaussian chirped pulses arranged in time as the spatial zone plates. Pulse-to pulse phases are chosen in opposition, since this structure is known to be more efficient in diffractive optics. Finally, and although the length of the spatial zone plates is progressive, the width of the individual pulses in the structure will be assumed equal. This assumption will lead to a more compact and realistic description of the effect, but also originates a saturation of the focusing process that has no spatial counterpart.

The plan of the paper is as follows. In section 2 we study the propagation of the structure, analysing the dispersion values necessary to attain focusing. The input structure transforms into a single pulse, which under certain conditions concentrates most of the energy of the input signal. Section 3 is devoted to analysis of the peak intensity of the focused pulse, assessing its dependence on the parameters that define the individual pulses, the accumulated dispersion and the timescale determining the focusing structure. In section 4 we study the width of the focused pulse and finally we end in section 5 with our conclusions.

2. Focusing condition

Let us consider pulse propagation in linear dispersive media carried by monochromatic waves of frequency ω_0. The equation governing the propagation of the complex pulse envelope, $\psi(z, t)$, in a dispersive medium at a distance z with negligible attenuation is [7, 28]

$$\frac{\partial \psi}{\partial z} = -\frac{\alpha}{2}\psi - \mathrm{i}\frac{\beta_2}{2}\frac{\partial^2 \psi}{\partial t^2}, \tag{1}$$

where $\beta(\omega) = \beta_0 + (\omega - \omega_0)\beta_1 + (\omega - \omega_0)^2\beta_2/2 + \cdots$ is the expansion of the dispersion relation about the carrier frequency, t is the time measured in the proper reference frame of the pulse, $t = t_{\mathrm{phy}} - \beta_1 z$, t_{phy} being the physical time, and α is the absorption coefficient. This equation describes the linear propagation of the pulse envelope, taking into account the attenuation, by means of the first term on the right side, and the first order dispersion of the medium by the second term. The absorption coefficient is assumed constant in the spectral range of work, so that the only effect it produces is a slight and uniform decrease of the signal intensity that does not affect the interference phenomenon. Therefore, we will not take it into account in our calculations hereafter. Dispersive propagation of coherent trains of pulses, as given by (1), is formally equivalent to paraxial propagation of waves in diffractive optics. The impulse response or propagation kernel of this linear system is the one-dimensional Fresnel diffraction kernel. In a dispersive medium of length L, this kernel is $h_\xi(t) = (-2\pi \mathrm{i}\xi)^{-1/2}\exp(-\mathrm{i}t^2/2\xi)$, where $\xi = \beta_2 L$ is the accumulated dispersion of the line. We will assume that the total bandwidth of the train of pulses lies inside a passband around the carrier where ξ can be assumed constant.

The input field is composed of two trains of pulses in phase opposition. In each of these trains, neighbouring pulses are separated in a quantity that is proportional to the square root of the natural numbers,

$$\begin{aligned}\psi_0(t) = f_0(t) &+ \sum_{n=1}^{M} f_0\left(t - t_0\sqrt{2n+1/2}\right) \\ &+ \sum_{n=1}^{M} f_0\left(t + t_0\sqrt{2n+1/2}\right) \\ &- \sum_{n=1}^{M} f_0\left(t - t_0\sqrt{2n-1/2}\right) \\ &- \sum_{n=1}^{M} f_0\left(t + t_0\sqrt{2n-1/2}\right),\end{aligned} \tag{2}$$

where t_0 is the scale of the temporal separation between different input pulses. The upper limit of the summation, M, gives the number of pulses of the train, N, through the expression $N = 4M + 1$, and the function f_0 expresses the initial pulse profile, which will be regarded as Gaussian with width t_p. C is the chirp or phase-modulation parameter:

$$f_0(t) = \exp\left[-(1 + \mathrm{i}C)t^2/2t_p^2\right]. \tag{3}$$

We will assume that the width of the pulses is smaller than the separation parameter, $t_p \ll t_0$, or equivalently that the linewidth $1/\tau = (1 + C^2)^{1/2}/t_p$ of the chirped pulses is bigger compared with the typical frequency separation between pulses in the train, $1/t_0$.

Figure 1 shows a comparison between the transmittance of a Fresnel phase zone plate (at the top of the figure) and the temporal amplitude distribution of the input train entering the dispersive line, equation (2) (at the bottom of the figure). The pulses of the input signal are arranged in time in the same way as the Fresnel zones of the zone plate. The main difference is that the widths of the pulses of the train remain constant, whereas the width of the Fresnel zones in the phase zone plate is proportional to the square root of the natural numbers. From the apparent analogy between both the input signal and the zone plate we expect the existence of pulse focusing after dispersive propagation, in analogy with the appearance of diffraction orders of a phase zone plate.

The propagation of the input envelope (2) through the linear system (1) yields a coherent sum of dispersed pulses,

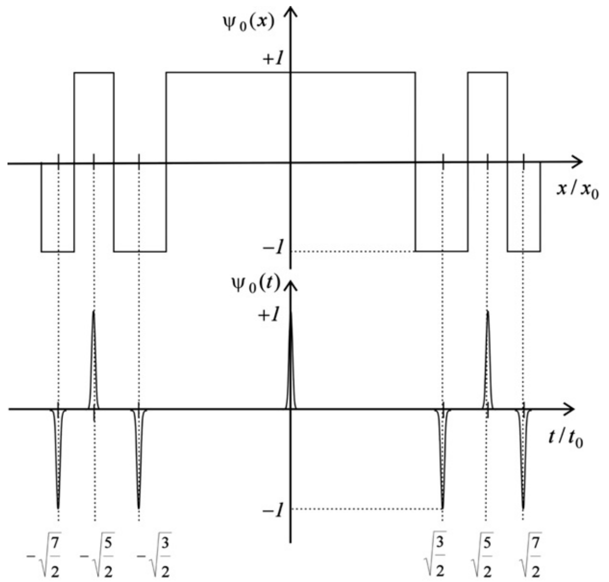

Figure 1. Input pulse structure in comparison with a spatial phase zone plane. (x_0 is the radius of the fist Fresnel zone.)

$$\psi_\xi(t) = f_\xi(t) + \sum_{n=1}^{M} f_\xi\left(t - t_0\sqrt{2n+1/2}\right) + \sum_{n=1}^{M} f_\xi\left(t + t_0\sqrt{2n+1/2}\right) - \sum_{n=1}^{M} f_\xi\left(t - t_0\sqrt{2n-1/2}\right) - \sum_{n=1}^{M} f_\xi\left(t + t_0\sqrt{2n-1/2}\right), \quad (4)$$

where $f_\xi(t)$ is the profile of the dispersed pulse:

$$f_\xi(t) = \frac{t_p}{\left(t_p^2 + \xi C - \mathrm{i}\xi\right)^{1/2}} \exp(-\kappa t^2/2), \quad (5)$$

and where we have introduced the complex parameter κ,

$$\kappa = \frac{1}{t_p^2 + 2\xi C + \xi^2/\tau^2} + \mathrm{i}\frac{\xi/\tau^2 + C}{t_p^2 + 2\xi C + \xi^2/\tau^2}. \quad (6)$$

The real part of κ is the inverse of the squared width of the dispersed pulse, whereas its imaginary part accounts for the chirp of the pulse after dispersion, see equation (5). Note that for $\xi \gg \tau^2$, i.e., for high accumulated dispersion, κ reduces to $(\tau/\xi)^2 + \mathrm{i}/\xi$ and therefore the dependence of the dispersed signal on the sign of chirp is subleading. The output envelope (4) can be written after some calculations as

$$\psi_\xi(t) = \frac{t_p \exp(-\kappa t^2/2)}{(t_p^2 + \xi C - \mathrm{i}\xi)^{1/2}} \left[1 + 2\exp(-\kappa t_0^2/4) \times \sum_{n=1}^{M} \exp(-n\kappa t_0^2)\cosh(\kappa t_0 t\sqrt{2n+1/2}) - 2\exp(\kappa t_0^2/4) \times \sum_{n=1}^{M} \exp(-n\kappa t_0^2)\cosh(\kappa t_0 t\sqrt{2n-1/2})\right], \quad (7)$$

where equation (5) has been used.

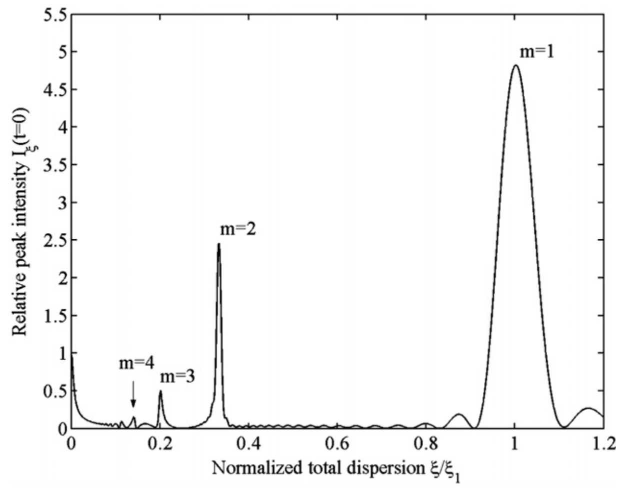

Figure 2. Relative output intensity at $t = 0$ versus ξ/ξ_1. Calculations have been made for $C = 0$; $N = 41$ and $t_0 = 30t_p$.

To compute the values of dispersion where pulse focusing is achieved, we must consider the relative phases between pulses after propagation. Then, setting $t = 0$ in equation (7) and leaving the dispersion parameter ξ as an indeterminate variable, we obtain

$$\psi_\xi(0) = \frac{t_p}{(t_p^2 + \xi C - \mathrm{i}\xi)^{1/2}} \times \left[1 - 4\sinh(\kappa t_0^2/4)\sum_{n=1}^{M}\exp(-n\kappa t_0^2)\right]. \quad (8)$$

Therefore all the dispersed pulses in this sum are cophasic at $t = 0$ and thus reinforce the peak value of the dispersed train, at those values of dispersion ξ such that $t_0^2\,\mathrm{Im}(\kappa) = 2\pi s$, with s any integer and $\mathrm{Im}(\kappa)$ the imaginary part of κ. However, for even values of s it is straightforward to notice that the hyperbolic sine that precedes the sum in (8) vanishes, and thus we are led to the following set of solutions:

$$t_0^2\,\mathrm{Im}(\kappa) = 2\pi(2m-1), \quad (9)$$

where m is an integer number that represents the dispersion order, in analogy with the diffraction orders in a phase zone plate. Substituting this value of the imaginary part of κ back into equation (8), we obtain the values of ξ_m that lead to the focusing of the train,

$$\xi_m = \frac{t_0^2}{4\pi(2m-1)} - C\tau^2 \pm \sqrt{\left(\frac{t_0^2}{4\pi(2m-1)}\right)^2 - \tau^4}. \quad (10)$$

This allowable set of solutions is associated with both positive and negative values of m, and with both positive and negative branches of the square root. To explore the physical solutions, let us consider the limit of high linewidth $\tau \to 0$. Then, formula (10) is equivalent to the formula of focus positions of the phase zone plate in diffractive optics,

$$\xi_m \approx \frac{t_0^2}{2\pi(2m-1)} = \frac{\xi_1}{2m-1}, \quad (11)$$

as long as the $\pm$ sign is chosen in accordance with the sign of $2m-1$. In formula (11) $\sqrt{\xi_1} = t_0/\sqrt{2\pi}$ is the principal

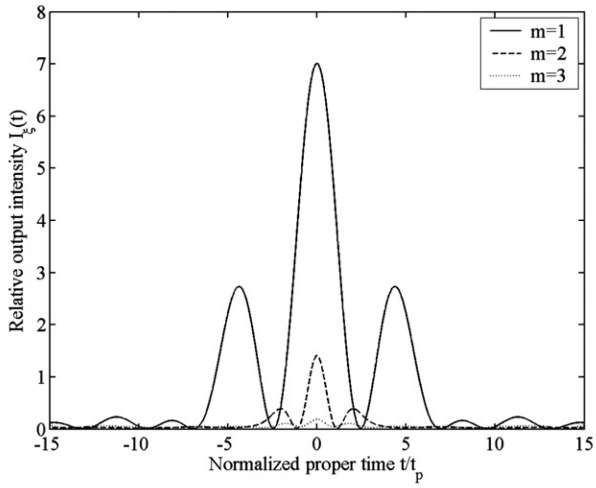

Figure 3. Relative output intensity in the dispersions orders $m = 1, 2$ and 3 when the input signal is formed by $N = 41$ pulses with $C = 0$ and $t_0 = 30t_p$.

focal time. Therefore we consider the positive branch of the square root in (11) with positive dispersion orders m, and the negative branch with dispersion orders $m = 0$ or negative. Both sets of solutions are equivalent, since the resulting values or dispersion differ only in sign. Notice finally that, since these values of dispersion are of the order of t_0^2, the high accumulated dispersion limit $\xi \gg \tau^2$ is equivalent to the high linewidth limit, $t_0 \gg \tau$.

The basic features of pulse focusing are shown in figures 2 and 3. In figure 2 we show the output relative intensity at $t = 0$, $I_\xi(0)$, given by the square module of equation (8), versus the normalized total dispersion ξ/ξ_1. The input signal consists of $N = 41$ unchirped pulses, and $t_0 = 30t_p$. Then the values of normalized dispersion, ξ/ξ_1, in the first four dispersion orders are 1, 1/3, 1/5 and 1/7 respectively, see equation (11), so that the output intensity presents relative maxima at these values of dispersion. Notice the high depth of focus of the first dispersion order. Also, we observe a rough decrease in intensity with increasing dispersion order. This points out that efficient focusing is only obtained for $m = 0$ or 1. The relative output intensity $I_\xi(t)$ for these values of dispersion, defined as the ratio between the peak intensity of the focused pulse $|\psi_\xi(t)|^2$ and the peak intensity of the individual pulses in the original train $|f_0(0)|^2$, is shown in figure 3. The pulse centred in $t = 0$ carries most of the energy of the total input signal. On both sides of the central pulse there are a series of symmetric lobes generated by destructive interference between the dispersed pulses, which carry the energy to be focused at the other diffraction orders, in analogy with the spatial zone plates. Side-lobe pulses can be suppressed in time domain by using a nonlinear loop mirror as an intensity discriminator [18]. The general analysis of pulse focusing as a function of the parameters that define the train is presented in the following sections.

3. Peak intensity

The relative peak intensity $I_\xi(0)$ can be analytically obtained from equations (3) and (7) at $t = 0$,

$$I_\xi(0) = \frac{q_\xi}{q_0}\left|1 + \mathrm{i}(-1)^m \frac{\exp(-q_\xi^2/2)}{\sinh(q_\xi^2/4)}\left[1 - \exp(-Mq_\xi^2)\right]\right|^2, \tag{12}$$

where we have defined the parameters

$$q_0 = \frac{t_0}{t_p}, \qquad \text{and} \qquad q_\xi = \frac{t_p t_0}{\sqrt{(t_p^2 + C\xi_m)^2 + \xi_m^2}}. \tag{13}$$

These parameters are a measure of the relative dimensions of the basic scale t_0 with respect to the temporal width of the input pulses f_0 and the dispersed pulses f_ξ, respectively. Notice that in the limit of high dispersion or high linewidth q_ξ can be approximated as $q_\xi \cong \tau t_0/\xi_m \cong 2\pi(2m-1)\tau/t_0 \ll 1$.

From equation (12), it follows that the intensity pulse of the focused pulse is higher as the second term in the sum increases, through the value of q_ξ. Moreover, the number of pulses in the train affects the peak intensity through M. Then, the behaviour of the peak intensity with the number of pulses can be divided into two regimes. In the first one, $M\,q_\xi^2 \ll 1$, the peak intensity increases as

$$I_\xi(0) \approx \frac{q_\xi}{q_0}\left(1 + \frac{\exp(-q_\xi^2)}{\sinh^2(q_\xi^2/4)} q_\xi^4 M^2\right), \tag{14}$$

and in the second one, $M\,q_\xi^2 \gg 1$, the peak intensity saturates, reaching an asymptotic value:

$$I_\xi(0)|_{\max} \approx \frac{q_\xi}{q_0}\left(1 + \frac{\exp(-q_\xi^2)}{\sinh^2(q_\xi^2/4)}\right). \tag{15}$$

When $q_\xi \ll 1$, i.e., in the limit of high linewidth or high dispersion, this maximum value of the peak intensity is

$$I_\xi(0)|_{\max} \approx \frac{16}{q_0 q_\xi^3} \approx \frac{2}{\pi^3}\frac{1}{|2m-1|^3}\frac{t_0^2}{\tau^2}\sqrt{1 + C^2}, \tag{16}$$

and therefore pulse focusing is only efficient in the first dispersive orders, $m = 0$ or 1.

Although (16) depends on both linewidth and chirp, the condition to reach saturation depends only on the linewidth. From equation (12), the number of pulses in the basic focusing structure necessary to reach saturation, $N_{\mathrm{SAT}} = 4M_{\mathrm{SAT}} + 1$, behaves as

$$N_{\mathrm{SAT}} \sim q_\xi^{-2} \propto \frac{1}{(2m-1)^2}\frac{t_0^2}{\tau^2}. \tag{17}$$

Therefore, the number of pulses to reach saturation depends only on the linewidth of the basic pulses (17), but the peak intensity, for a given value of linewidth, increases with the chirp of the pulses (16). The saturation can be explained as follows. Since the width of the pulses in the focusing structure is the same along the input signal, pulses separated from the central one will tend to lie closer as the total number of pulses increases. When this happens, the most external pulses cannot contribute to focusing and the peak intensity in a given dispersion order saturates.

In figure 4 the relative peak intensity of the focused pulse, equation (12), in the dispersive order $m = 1$ is depicted as a function of the total number of pulses in the train, N. In the

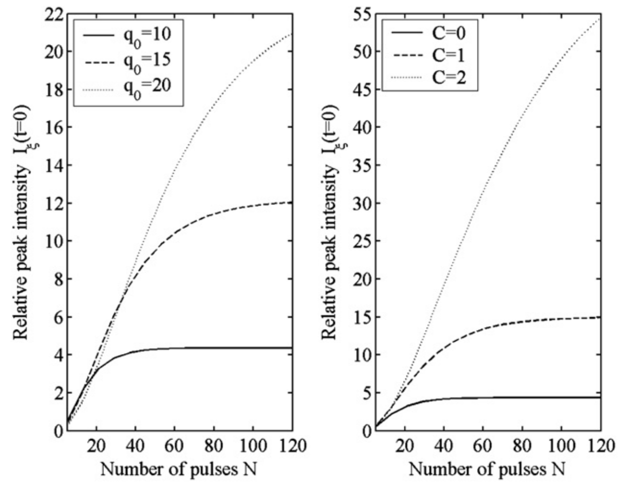

Figure 4. Relative peak intensity versus number of pulses in the first dispersion order $m = 1$. The parameters are $C = 0$ and $q_0 = 10$, 15 and 20 (left figure) and $q_0 = 10$ and $C = 0$, 1 and 2 (right figure).

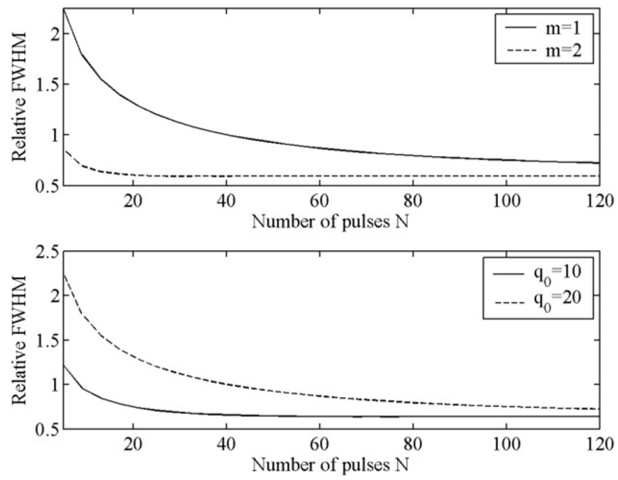

Figure 5. Relative FWHM versus number of pulses. The parameters are $C = 0$, $q_0 = 20$ and $m = 1$ and 2 (above), and $C = 0$, $m = 1$ and $q_0 = 10$ and 20 (below).

left picture, the input pulses are unchirped and $q_0 = 10$, 15 and 20 so that $q_\xi = 0.63$, 0.42 and 0.32 respectively, and on the right $q_0 = 10$ and $C = 0$, 1 and 2, so that $q_\xi = 0.63$, 0.44 and 0.28. On the left, the different regimes, initial parabolic growth and subsequent saturation, are apparent. We also observe the increase in the number of pulses for saturation, as we expected from the dependence of (17) on the squared ratio t_0/τ. Moreover, the maximum values of the relative peak intensity, given by equation (15) (4.4, 12.2, and 23.4 for $q_0 = 10$, 15 and 20 respectively), are in accordance with our simulation in figure 4.

When the input pulses are chirped, the linewidth is increased, so that the saturation occurs for higher values of N, as observed on the right-hand side of figure 4. Moreover the peak intensity for chirped pulses reaches higher values as we expect from equation (16). For example, we obtain a relative output peak intensity of about 7 from an input with a basic focusing structure of 21 pulses, whereas it is about 3.2 for unchirped pulses. Therefore, we conclude that the focusing process is much more efficient if the individual pulses of the focusing structure are chirped, even if saturation is not reached.

4. Width

The basic properties of the width of the focused pulses can be extracted from the coherent sum (7). The real part of the complex argument of the hyperbolic cosine in the summation yields a smooth function, whereas the imaginary part yields an oscillatory one. The frequency of these oscillatory functions increases with the square root index of the summation, $\sqrt{n}$. When $t = 0$, the oscillatory functions tend to unity for all values of n, and therefore the output signal takes the maximum value, equation (8). As t departs from zero, the interference of oscillatory functions with different frequencies produces a decrease in the intensity of the focused pulse, in a such a way that the leading contributions to the output signal around $t = 0$ are achieved if the argument of the oscillatory functions remains stationary below a threshold value, that is

$$t t_0 \sqrt{2n \pm 1/2}\, \mathrm{Im}(\kappa) < \text{const}. \tag{18}$$

The most unfavourable case for the above relation occurs when n achieves the maximum value in the upper limit of the summation, $n = M$, since this case corresponds to the highest oscillatory frequency in the coherent sum (8). Then, the greatest value of t that satisfies the bound given in equation (18) when $n = M$ represents a measure of the width Δt of the output pulse. Noticing that $N \propto M$, we obtain the following dependence of the pulse width of the focused pulse relative to the initial width of the pulses and the total number of pulses:

$$\frac{\Delta t}{t_p} \propto \frac{1}{|2m-1|} \frac{q_0}{\sqrt{N}}, \tag{19}$$

where equations (18) and (9) have been used.

From equation (19) it follows that the relative width increases linearly with the parameter $q_0 = t_0/t_p$, and thus with the reparation parameter t_0. It is also inversely proportional to the dispersion order and to the square root of the number of pulses. In practice, it is customary to use the full width at half maximum (FWHM) to estimate the width of the pulse. In figure 5 we represent the numerically computed FWHM of the focused pulse in different dispersive orders, normalized by the FWHM of the input pulses, versus the number of pulses of the basic focusing structure. In the top figure the parameters are $q_0 = 20$ and $m = 1$ and 2. Due to the inverse dependence of the relative FWHM on the dispersion order, focused pulses are efficiently compressed for a moderate number of pulses only when higher dispersion orders are used, $m \neq 0$, 1. However, the use of higher dispersive orders provides low peak intensities, as shown in the previous section. Therefore, the use of this dispersive structure is not an efficient tool to generate compressed pulses. Below, the dependence of the relative FWHM with respect to the number of pulses is illustrated for the first dispersion order $m = 1$ and different values of the parameters $q_0 = 10$ and 20. Alternatively, and due to the structure of (19), the focused pulse width can be reduced in the first dispersion order by decreasing the temporal separation t_0 of the focusing structure.

Another feature observed in the simulations in figure 5 is the saturation of the compression factor, i.e., the focused

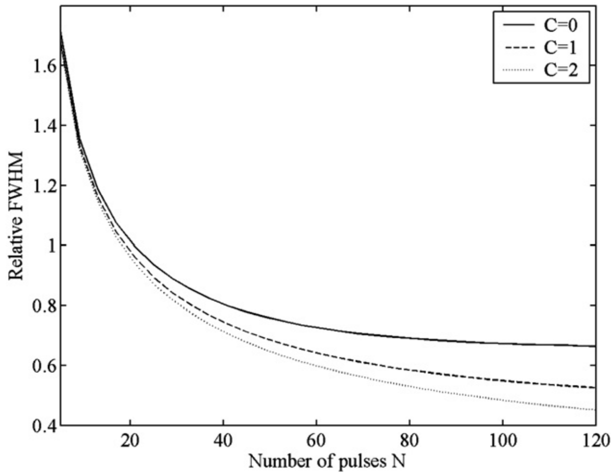

Figure 6. Relative FWHM versus number of pulses in the first dispersion order $m = 1$. The parameters are $q_0 = 15$ and $C = 0$, 1 and 2.

pulse width does not tend asymptotically to zero. This is to be expected since $N_{\rm SAT}$ determines the maximum number of pulses that contribute to the focusing process. In figure 6 the numerically computed FWHM is depicted as a function of the number of pulses. The parameters of the input train are $q_0 = 15$, $m = 1$ and $C = 0$, 1 and 2. In this figure we observe two regimes. For moderate number of pulses ($N < 20$), the width of the output pulse decreases with N and does not depend on the chirp parameter, as equation (19) indicates. However, since $N_{\rm SAT}$ increases with chirp and the relative FWHM decreases until $N \approx N_{\rm SAT}$, the output FWHM width reaches asymptotically lower values the higher is the chirp parameter.

5. Conclusions

In this paper we have studied the propagation of a progressive structure of Gaussian chirped pulses in phase opposition through a dispersive line, as a method to produce a focused pulse by means of a coherent sum of dispersed pulses. This structure has been devised using a simple analogy with a diffractive phase zone plate. Notice that we have chosen the analogy of a phase zone plate only as an example in our calculations, and equivalent results are obtained with an amplitude zone plate. The input structure focused into a single pulse for certain values of dispersion, due to constructive interference between the dispersed pulses of the structure. We have characterized the output-focused pulse, which in general carries side-lobe pulses associated with light focusing in different dispersion orders.

The peak intensity and the width of the focused pulse have also been characterized, analysing its dependence on the accumulated dispersion, the temporal separation that defines the focusing structure, and also the parameters of the individual pulses in the input structure. Pulse focusing is only efficient in the first dispersion order, and the width of the focused pulse is lower than but of the same order of magnitude as the width of the individual pulses of the focusing structure. The peak intensity can reach values of the order of ten times the individual pulse peak intensity for moderate number of pulses in the focusing structure.

The technique presented here applies to any coherent pulse burst waveform of the type presented in equation (2), since it is based on the coherent interference of the dispersed pulses of the original burst. Therefore, it can be applied to bursts composed of pico- or subpicosecond pulses. The only technical limitation is the necessity of a first-order dispersive medium with sufficient bandwidth to cope with the optical spectrum of the burst. On the other hand, the main limitation of the proposed pulse focusing method is the generation of a train of coherent pulses with a complex structure like the one presented in (2). An obvious possibility is the direct shaping of the train envelope by electro-optic modulation [29–31]. This technique allows the patterning of structures with resolution of some tens of picoseconds over a range of nanoseconds. Waveform generation with 10 ps resolution has been demonstrated by use of direct Fourier-space synthesis by phase locking independent lasers [32] and weighted optical delay lines [33]. However, arbitrary optical waveform generation with subpicosecond resolution requires the spectral shaping of broadband optical sources [34, 35]. Using this technique, Chou *et al* [36] and Wefers *et al* [37] have generated pulse bursts whose duration and separation is progressively smaller. It is remarkable that with these bursts the saturation of the pulse focusing explained in the text will not take place and therefore it is possible that the values of the intensity of the pulse achieved from this structure are higher than from the input train we have proposed.

Acknowledgments

This work has been supported by Ministerio de Educación y Ciencia, Spain, under project TIC2003-03041. L Chantada is also supported by Ministerio de Educación y Ciencia, Spain, through a Formación del Profesorado Universitario grant. L Chantada's e-mail is falaura@usc.es. The authors thank the referees for their comments and suggestions.

References

[1] Papoulis A 1994 *J. Opt. Soc. Am.* A **11** 3–13
[2] Kolner B H 1994 *IEEE J. Quantum Electron.* **30** 1951–63
[3] Saleh B E A and Teich M C 1991 *Fundamentals of Photonics* (New York: Wiley)
[4] Tournois P 1964 *C. R. Acad. Sci. Paris* **258** 3839–42
[5] Tournois P, Vernet J L and Bienvenu G 1968 *C. R. Acad. Sci. Paris* **267** 375–8
[6] Bennett C V and Kolner B 2000 *IEEE J. Quantum Electron.* **36** 430–7
[7] Agrawal G P 2001 *Nonlinear Fiber Optics* 3rd edn (San Diego, CA: Academic)
[8] Agrawal G P 2001 *Applications of Nonlinear Fiber Optics* 3rd edn (San Diego, CA: Academic) chapter 6
[9] Kolner B H and Nazarathy M 1989 *Opt. Lett.* **14** 630–2
[10] Kolner B H 1997 *J. Opt. Soc. Am.* A **14** 3349–57
[11] Bennett C V and Kolner B H 1999 *Opt. Lett.* **11** 783–5
[12] Jiang L E, Grein M E, Haus H A, Ippen E P and Yokohama H 2003 *Opt. Lett.* **28** 78–80
[13] Bjorkholm J E, Turner E H and Pearson D B 1975 *Appl. Phys. Lett.* **26** 564–6
[14] Wigmore J K and Grischkowsky D R 1978 *IEEE J. Quantum Electron.* **14** 310–5

[15] Jannson T 1983 *Opt. Lett.* **8** 232–4
[16] Muriel M A, Azaña J and Carballar A 1999 *Opt. Lett.* **24** 1–3
[17] Azaña J, Chen L R, Muriel M A and Smith P W E 1999 *Electron. Lett.* **35** 2223–4
[18] Azaña J, Berger N K, Levit B and Fischer B 2004 *IEEE Photon. Technol. Lett.* **16** 882–4
[19] Mashall W K, Paslaski J and Yariv A 1996 *Appl. Phys. Lett.* **68** 2496–8
[20] Mashall W K and Yariv A 2000 *IEEE Photon. Technol. Lett.* **12** 302–4
[21] Hakimi H, Hakimi F, Hall K L and Rauschenbach K A 1999 *IEEE Photon. Technol. Lett.* **11** 1048–50
[22] Jannson T and Jannson J 1981 *J. Opt. Soc. Am.* **71** 1373–6
[23] Andrekson P A 1993 *Opt. Lett.* **18** 1621–3
[24] Azaña J and Muriel M A 2001 *IEEE J. Sel. Top. Quantum Electron.* **7** 728–44
[25] Longhi S, Marano M, Laporta P and Prunei V 2000 *IEEE Photon. Technol. Lett.* **12** 1498–500
[26] Berger N K, Vodonos B, Atkins S, Smulakovsky V, Bekker A and Fischer B 2003 *Opt. Commun.* **217** 343–9
[27] Ojeda-Castañeda J and Gómez-Reino C 1996 *Selected Papers on Zone Plates* (*SPIE Mileston Series* vol MS 128) (Bellingham, WA: SPIE Optical Engineering Press) and references therein
[28] Saleh B E A and Teich M C 1991 *Fundamentals of Photonics* (New York: Wiley)
[29] Haner M and Warner W S 1987 *Appl. Opt.* **26** 3687–94
[30] Burkhart S C and Wilcox R B 1990 *IEEE Trans. Microw. Theory Tech.* **38** 1514–8
[31] Skeldon M 2002 *J. Opt. Soc. Am.* B **19** 2423–6
[32] Shen M and Minasian R A 2004 *IEEE Photon. Technol. Lett.* **16** 1155–7
[33] Hyodo M, Onodera N and Abedin K S 1999 *Opt. Lett.* **24** 303–5
[34] McKinney J D, Seo D, Learird D E and Weiner A M 2003 *J. Lightwave Technol.* **21** 3020–8
[35] Azaña J and Chen L R 2002 *J. Opt. Soc. Am.* B **19** 2758–69
[36] Chou J, Han Y and Jalali B 2003 *IEEE Photon. Technol. Lett.* **15** 581–3
[37] Wefers M M and Nelson K A 1995 *Opt. Lett.* **20** 1047–9